

Thermal Denaturation of Myoglobin in Water–Disaccharide Matrixes: Relation with the Glass Transition of the System

Giuseppe Bellavia, Grazia Cottone, Sergio Giuffrida, Antonio Cupane, and Lorenzo Cordone*

Dipartimento di Scienze Fisiche ed Astronomiche, Università di Palermo and CNISM, Via Archirafi 36, Palermo, Italy I-90123

Received: May 4, 2009; Revised Manuscript Received: July 2, 2009

Proteins embedded in glassy saccharide systems are protected against adverse environmental conditions [Crowe et al. *Annu. Rev. Physiol.* **1998**, 60, 73–103]. To further characterize this process, we studied the relationship between the glass transition temperature of the protein-containing saccharide system (T_g) and the temperature of thermal denaturation of the embedded protein (T_{den}). To this end, we studied by differential scanning calorimetry the thermal denaturation of ferric myoglobin in water/disaccharide mixtures containing nonreducing (trehalose, sucrose) or reducing (maltose, lactose) disaccharides. All the samples studied are, at room temperature, liquid systems whose viscosity varies from very low to very large values, depending on the water content. At a high water/saccharide mole ratio, homogeneous glass formation does not occur; regions of glass form, whose T_g does not vary by varying the saccharide content, and the disaccharide barely affects the myoglobin denaturation temperature. At a suitably low water/saccharide mole ratio, by lowering the temperature, the systems undergo transition to the glassy state whose T_g is determined by the water content; the Gordon–Taylor relationship between T_g and the water/disaccharide mole ratio is obeyed; and T_{den} increases by decreasing the hydration regardless of the disaccharide, such effect being entropy-driven. The presence of the protein was found to lower the T_g . Furthermore, for nonreducing disaccharides, plots of T_{den} vs T_g give linear correlations, whereas for reducing disaccharides, data exhibit an erratic behavior below a critical water/disaccharide ratio. We ascribe this behavior to the likelihood that in the latter samples, proteins have undergone Maillard reaction before thermal denaturation.

Introduction

Biopreservation is a relevant topic, in particular for its technological implications in the food industry, pharmaceuticals, and medicine.¹ In an aqueous environment, cosolvents such as disaccharides cause an increase in the thermal denaturation temperature of proteins' thermal denaturation.² Furthermore, glassy saccharide matrixes protect biostructures against adverse conditions, such as a very dry environment, high or low temperature.³ The molecular mechanisms behind this effect are not yet fully understood and are still matter of debate. Among saccharides, trehalose (see Figure 1) is the best stabilizer of biostructures commonly found in nature.^{4,5} Several hypotheses have been proposed to explain the origin of this peculiarity: according to the *water replacement hypothesis*,⁶ trehalose stabilization occurs via the formation of hydrogen bonds (HBs) between the disaccharide and the biostructure in the dry state. This hypothesis has been suggested to be at the basis of membranes' bioprotection by trehalose.^{7–10} The *water entrapment hypothesis*¹¹ proposes that trehalose, rather than directly binding to biomolecules, entraps the residual water at the interface by glass formation, thus preserving the native solvation. This model is based on extrapolation of thermodynamic data by Timasheff and co-workers,^{2,12} who suggested that, in solution, the cosolvent is preferentially excluded from the protein domain, different cosolvents being classified on a scale from more preferentially bound to more preferentially excluded, the latter better stabilizing the protein structure. Disaccharides are among the most excluded cosolvents, trehalose being at the top of the

scale.² However, the mechanism by which trehalose stabilizes biomolecules in a water-excess medium¹¹ is likely to be different from the mechanism under low-water conditions.^{13,14}

A different, non-mutually exclusive approach to explain trehalose peculiarity focuses on the high viscosity of the glassy host medium,¹³ which causes motional inhibition and hindering of processes leading to loss of structure and denaturation. In this respect, Green and Angell¹⁴ suggested the peculiarity of trehalose to be related to its rather high glass transition temperature with respect to other glass-forming disaccharides. Indeed, protein dynamics is highly inhibited when the protein is embedded in a trehalose glassy matrix,^{15–35} the inhibition being markedly dependent on the traces of residual water.^{28,32,35–37} It has also been reported that solvent viscosity is responsible for the reduction of anharmonic motions and for the slowing down of conformational relaxations of proteins encapsulated in silica hydrogels.^{38–40}

Molecular dynamic (MD) simulations^{41,42} have suggested that in low-water trehalose matrixes, the protein is confined within a HB network that includes water molecules connecting groups at the protein surface to the surroundings. The same simulation also showed that the fraction of water molecules involved in such networks increases upon decreasing the water content, so as the number of bonds in which each water molecule is involved. These findings led to the suggestion that the rigidity of the network increases by lowering the water content and that this network is mainly responsible for coupling the internal dynamics of the protein to that of the low-water matrix.^{28,33,35} In this context, the inhibition of internal protein dynamics under

* Corresponding author. Phone: +39-0916234215. Fax: +39-0916162461. E-mail: cordone@fisica.unipa.it.

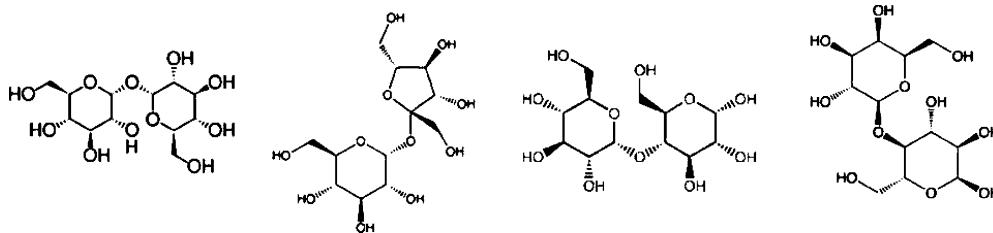


Figure 1. From left: the trehalose, sucrose, maltose, and lactose molecules.

conditions of extreme drought can be explained in terms of a tight anchorage of the protein surface to a stiff matrix.^{28,33,35}

This hypothesis is in line with the water-entrapment hypothesis.¹¹ Indeed, as shown by MD results,⁴¹ water at the protein surface is in excess with respect to the average solvent composition, whereas relatively few sugar molecules are bound to the protein. Therefore, MD simulations⁴² suggest that, at variance with water entrapment, the ability of the sugar to protect biomolecules is not simply related to the preservation of the native solvation, but that it arises from the ability to lock the protein surface through constrained water molecules, which hinder motions. Accordingly, when strong, extended HB networks form, as in glassy trehalose–water–protein systems, the energy penalty associated with the solvent rearrangements, which is needed to accommodate large scale protein motions, increases sizably,²⁶ as recently supported by vibrational echo experiments and MD simulations performed on different heme proteins in trehalose glasses and silica gels.^{24,25}

In this respect, it has been suggested that water translational motions,^{43–45} which allow complete exchange of protein-bound water molecules by translational displacement, are necessary for large-scale fluctuations involving displacements of the protein surface,⁴⁶ such as interconversion among high tier substates and structural relaxations. Furthermore, the same authors^{43–45} have suggested that exchange of protein–water HBs by water rotational/librational motions, not sufficient to permit large-scale internal motions, still allows interconversion among low-tier conformational substates.

Coupling based on HB networks might not take place in other disaccharide glassy matrixes; in particular, at variance with trehalose, lack of coupling was found for the photosynthetic reaction center from the purple bacterium *Rhodobacter sphaeroides* in very dry sucrose, where a local protein–matrix nanophase separation has been observed at a water/disaccharide mole ratio lower than 0.8.³³ Phase separation has been also observed in lactose, but not in trehalose, in a study on lysozyme–disaccharide systems.⁴⁷

Recently, a differential scanning calorimetry (DSC) study reported that, in myoglobin–trehalose–water systems at a water/disaccharide ratio in which homogeneous glasses can be obtained, a linear correlation exists between the protein denaturation temperature, T_{den} , and the glass transition temperature, T_g , of the whole protein–trehalose–water system.⁴⁸ This gave further information on the coupling between the protein stability and the dynamics of the surrounding matrix. In this work, we extended the analysis to obtain detailed information on the thermodynamics involved in the stabilization processes and performed analogous DSC measurements on a further nonreducing disaccharide (sucrose) and on two reducing disaccharides (maltose, lactose).

Materials and Methods

Samples. Trehalose (α -D-glucopyranosyl- α -D-glucopyranoside) from Hayashibara Shoji (Hayashibara Shoji Inc., Okayama,

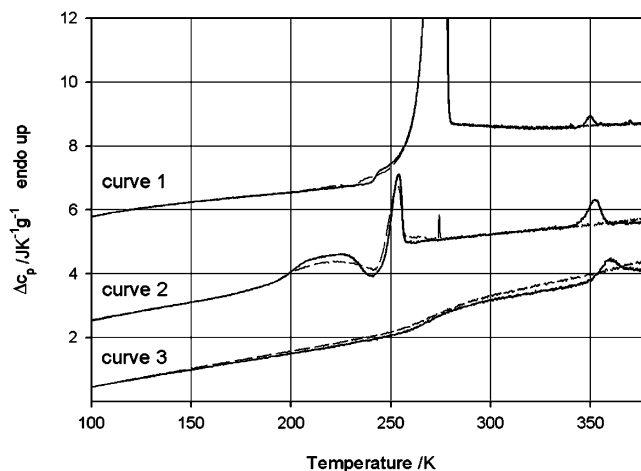


Figure 2. Typical C_p -vs-temperature curves for myoglobin–disaccharide–water systems normalized to sample mass.⁴⁸ Curves are shifted for the sake of clarity. Curves 1–3: 270, 17, 4 water/trehalose mole ratio. Solid lines, first scan; dashed lines, second scan (after protein denaturation). Note that the normalization to the sample mass leads to different areas for the denaturation peaks.

Japan) was used after recrystallization from aqueous solutions. Lyophilized ferric horse myoglobin, sucrose (α -D-glucopyranosyl-(1 \leftrightarrow 2)- β -D-fructofuranoside), and maltose (4- O - α -D-glucopyranosyl-D-glucopyranose) were purchased from Sigma (Sigma, St. Louis, MO) and used without further purification. Lactose (4- O - β -D-galactopyranosyl-D-glucopyranose) was purchased from Galeno (Galeno, Comeana, Italy) and used without further purification. For sample preparation, myoglobin was dissolved (5×10^{-3} M) in a solution containing 2×10^{-1} M disaccharide and 2×10^{-2} M phosphate buffer (pH 7 in water) so that a constant ratio between disaccharide and myoglobin is achieved, equal to an ~ 40 disaccharide/myoglobin mole ratio. An aliquot (20 μ L) of the above solution was deposited in an aluminum pan for a volatile sample with a maximum volume of 20 μ L and a mass of about 23 mg. Then the sample was blow-dried at 55 $^{\circ}$ C until a suitable water concentration was achieved. The water content was estimated by weighting the sample before and after the blow-drying. Further depositions of solution and blow-drying were performed to obtain samples with water content from ~ 300 to ~ 2 water/disaccharide ratios and a myoglobin content of about 5 mg. The aluminum pans were then sealed.

Measurements. Calorimetric measurements were performed by a Diamond DSC PerkinElmer with a Cryofill device. Indium was used to calibrate the temperature and heat flow. The heat flow error was 0.05 mW. The temperature program consisted of two identical cycles performed as follows: cooling from 303 to 95 K at 500 K min^{-1} , holding 3 min, then warming to 393 K at 10 K min^{-1} . An empty sealed pan was used as a reference. To check the baseline stability and to match the aluminum mass contribution, a temperature cycle on a second empty pan was performed after each measurement.

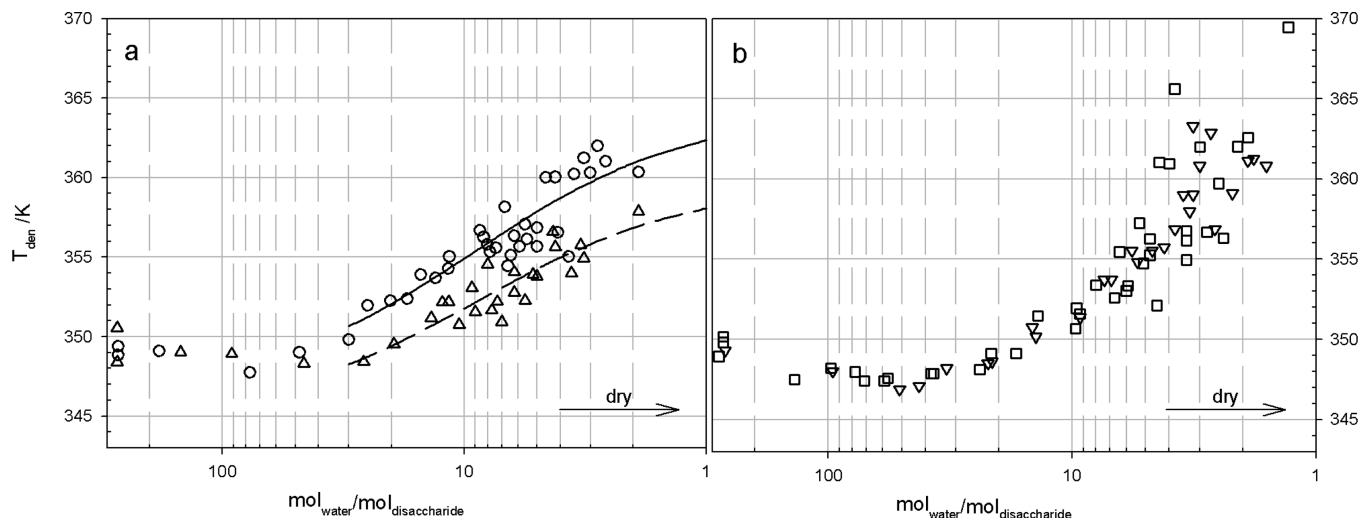


Figure 3. Denaturation temperature of myoglobin as a function of hydration. Panel a: in trehalose (circle)⁴⁸ and in sucrose (triangle up) systems. Panel b: in maltose (square) and in lactose (triangle down) systems. Lines are fittings in terms of eq 3.

The specific heat variation was evaluated by subtracting the heat flow measured by using empty aluminum pans, normalized to the pan mass, then dividing by the scan rate and the sample mass. After subtraction of a suitable cubic polynomial baseline,⁴⁹ the myoglobin denaturation temperature (T_{den}) was determined from the position of the irreversible endothermic peak and the denaturation enthalpy (ΔH_{den}) from its area. The temperature value at the onset of the leap of specific heat, at low temperature, characterized the glass transition temperature (T_g).

Results and Discussion

Typical upscan thermograms of protein–disaccharide–water systems at different water/disaccharide mole ratios are shown in Figure 2. We recall that in all experiments, the disaccharide/protein molar ratio is kept constant at ~ 40 . Three different regimes are distinguished: high water content, in which a small ΔC_p step (attributed to a glass transition) is followed by a large water melting peak that dominates the thermograms; intermediate water content, in which a glass transition followed by crystallization/melting peaks is observed; and low water content, in which only a glass transition occurs. In all cases, the thermograms show an irreversible melting peak at high temperatures, attributable to myoglobin denaturation.

Figure 3a and b shows the denaturation temperature of myoglobin in nonreducing (trehalose,⁴⁸ sucrose) and in reducing (maltose, lactose) disaccharide–water systems, respectively, as a function of the water/disaccharide molar ratio. As indicated by the arrow in the figures, the water content (hydration) decreases from left to right. For all the disaccharides investigated, T_{den} has a very weak hydration dependence at high water content, down to ~ 30 water/disaccharide; at lower hydrations, a relevant, disaccharide specific, T_{den} increase is observed. For nonreducing disaccharides, the T_{den} increase is monotonic and steeper for trehalose than for sucrose, in line with the well-known peculiarity of trehalose as protein stabilizer.³

The T_{den} increase at low water content is analogous to what is observed in binary water–protein systems, which show a strong dependence of protein stability on hydration, starting at protein-specific hydration levels.⁵⁰ For reducing disaccharides, the T_{den} increase is monotonic only up to ~ 5 water/disaccharide, whereas, at still lower hydrations, its behavior apparently becomes erratic. For some samples (e.g., maltose at a 1:4 water/disaccharide mole ratio), very high protein denaturation temperatures are observed, in the range 355–370 K.

At variance with our results, a sizable T_{den} increase has been observed, even at high hydration, by Timasheff and co-

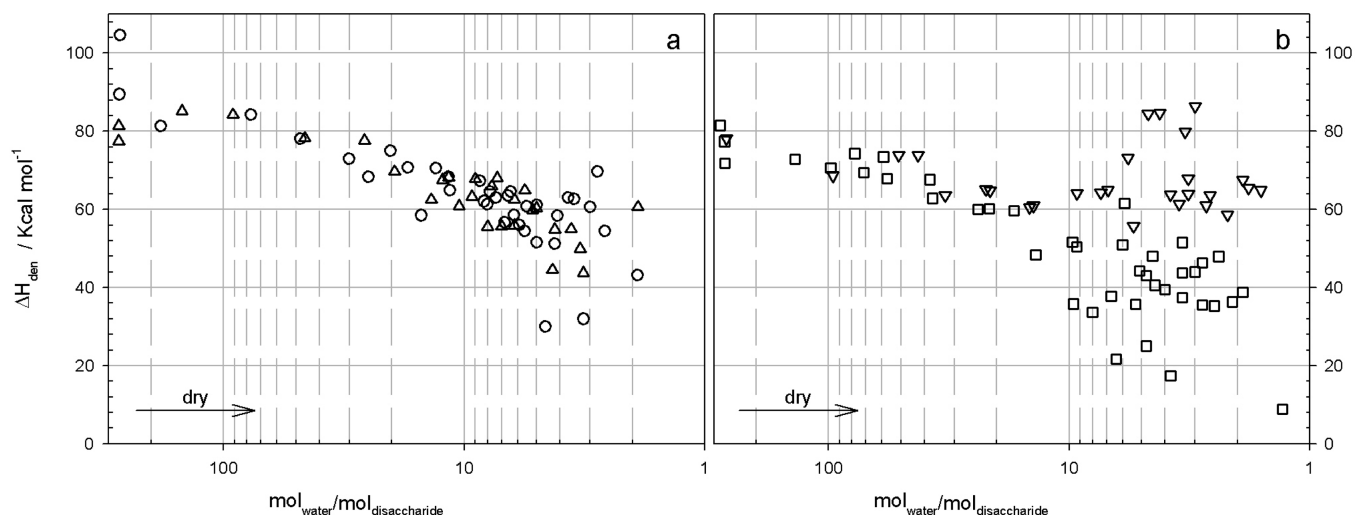


Figure 4. Denaturation enthalpy of myoglobin as a function of hydration. Panel a: trehalose⁴⁸ and sucrose. Panel b: maltose and lactose. Symbols as in Figure 3.

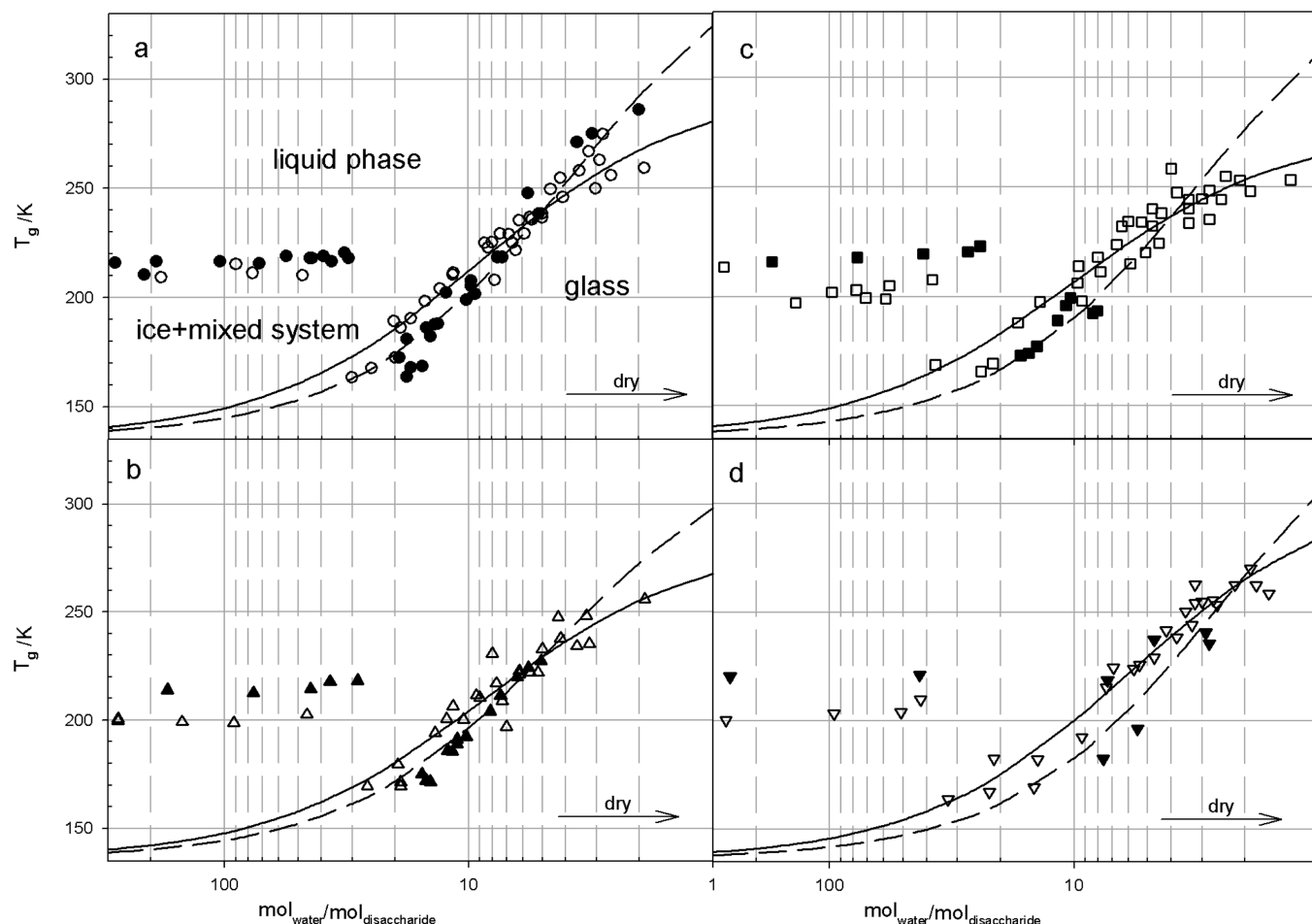


Figure 5. Glass transition temperature as a function of hydration in Mb–disaccharide–water systems (empty symbols and continuous lines) in comparison with the correspondent binary disaccharide–water systems (solid symbols and dashed lines). Lines are fittings in terms of the Gordon–Taylor formula (eq 1 in the text). Panel a: trehalose (circles).⁴⁸ Panel b: sucrose (triangles up). Panel c: maltose (squares). Panel d: lactose (triangles down).

workers,⁵¹ who studied RNase–trehalose samples from large dilution to ~ 50 water/disaccharide. We attribute this discrepancy to the widely different disaccharide/protein mole ratios used (~ 40 in our samples as compared to ~ 1300 to ~ 12000 in Timasheff's) or the sizable structural differences between RNase and Mb. Indeed, it has been reported that trehalose preferentially binds to GLU, ASP, and LYS at the protein surface:⁴² Mb is richer in these residues than RNase.

Figure 4a and b shows the denaturation enthalpy (ΔH_{den}) of myoglobin as a function of the water/disaccharide molar ratio. ΔH_{den} decreases on drying and keeps similar values for the nonreducing disaccharides, whereas for lactose, it is almost not dependent on hydration. By definition, the ratio $\Delta H_{\text{den}}/T_{\text{den}}$ is the denaturation entropy (ΔS_{den}). Since T_{den} increases by lowering the water content while ΔH_{den} decreases, it follows that ΔS_{den} decreases more rapidly than ΔH_{den} . This makes the stability increase of myoglobin in water/disaccharide matrixes at low hydrations an entropy-driven process; that is, decreasing the water content affects the protein–matrix interactions so that the reduction of the degeneracy of the unfolded state dominates the free energy differences between the folded and the unfolded state.

In Figure 5a–d, we report the glass transition temperatures of the systems as a function of the water/disaccharide molar ratio for both binary and ternary systems. These plots represent the state diagram of the systems: as indicated in Figure 5a, the upper region identifies the liquid state, and the lower region is

divided into two different states, corresponding to ice + mixed systems at high water content and the glassy state at low water content. The break at the 30 water/disaccharide mole ratio is the threshold between the glassy and ice + mixed system phases, consistent with our cooling rate (see below). The plots in ternary systems exhibit a behavior similar to what is observed in water–cosolvent binary systems.⁵² At low water content, where only glass transition occurs (see Figure 2, curve 3), the systems are homogeneous, and the glass transition temperature depends on hydration following the Gordon–Taylor expression,⁵³

$$T_g(f) = \frac{T_g(f \rightarrow 0) + T_g(f \rightarrow \infty) k \frac{MW_w}{MW_s} f}{1 + k \frac{MW_w}{MW_s} f} \quad (1)$$

where MW_w and MW_s are the water and disaccharide molecular weights, respectively; f is the water/disaccharide molar ratio; $T_g(f \rightarrow 0)$ and $T_g(f \rightarrow \infty)$ are the glass transition temperatures of the system in the absence of water and of disaccharide, respectively; and k is the nonlinearity parameter.⁵³

At high hydration levels, the systems are inhomogeneous, and a large part of the water crystallizes (see Figure 2, curve 1), whereas only a small fraction of the system vitrifies at a constant water/disaccharide molar ratio corresponding to the

TABLE 1: Parameters Obtained from Fittings of T_g vs Water/Disaccharide Molar Ratio in Terms of the Gordon–Taylor Expression (eq 1 in the text)

disaccharide	$T_g(f \rightarrow 0)/K$ (binary ^a)	$T_g(f \rightarrow 0)/K$ (ternary)	k (binary)	k (ternary)
trehalose	373	297 ± 13	4.9 ± 0.4	2.1 ± 0.5
sucrose	335	283 ± 16	4.6 ± 0.3	2.2 ± 0.6
maltose	368	277 ± 12	6.1 ± 0.8	1.9 ± 0.5
lactose	374	309 ± 17	7.8 ± 2.6	3.3 ± 0.8

^a Values taken from ref 55.

maximally freeze-concentrated solute matrix (C_g'),⁵² which in our samples is between a 10 and 7 water/disaccharide mole ratio. As a consequence, a constant T_g is observed (T_g').⁵² Under our cooling conditions, the systems obey the Gordon–Taylor equation also beyond C_g' , up to an ~ 30 water/disaccharide mole ratio. Interestingly, this hydration value corresponds to the onset of the T_{den} increase. We notice that in protein–trehalose–water systems, the T_g value at ~ 2 water molecules per disaccharide is ~ 270 K. This is comparable to the value at which in myoglobin, large scale motions, which involve displacement of the protein surface, appear.^{28,30}

In Figure 5, the fittings in terms of eq 1 are reported as solid and dashed lines for ternary (protein–disaccharide–water) and binary systems (disaccharide–water), respectively. In the fits, $T_g(f \rightarrow \infty)$ has been assumed to be the glass transition temperature of pure water (136 K, from ref 54), and the $T_g(f \rightarrow 0)$ has been fixed to the value of the pure disaccharide for binary systems.^{55–57} Indeed, it was difficult to obtain reliable values for $T_g(f \rightarrow 0)$ by a fitting procedure due to the lack of binary data in the low hydration region. Furthermore, the fitting of ternary data was very poor when using the $T_g(f \rightarrow 0)$ value for a binary system.^{55–57} For this reason, it has been left as a free-fitting parameter for ternary systems.

Results are reported in Table 1. For all the disaccharide investigated, the effect of the protein is to decrease both the k and the $T_g(f \rightarrow 0)$ values. The $T_g(f \rightarrow 0)$ decrease is indicative that, for $f \rightarrow 0$, looser water/disaccharide interactions are present: the protein, competing for water with disaccharide molecules,⁴² reduces the strength of the HB network encompassing the sample.

Figure 6a and b shows the denaturation temperature of Mb versus the glass transition temperature of the ternary systems; a linear correlation is evident between T_g and T_{den} in trehalose⁴⁸ and in sucrose (Figure 6a). The linearity can be expressed as

$$T_{den}(T_g) = T_{den}(f \rightarrow \infty) + \frac{\partial T_{den}}{\partial T_g} [T_g - T_g(f \rightarrow \infty)] \quad (2)$$

where $T_{den}(f \rightarrow \infty)$ is the T_{den} value extrapolated at $T_g(f \rightarrow \infty)$ (i.e. at the glass transition temperature of pure water, 136 K) and $\partial T_{den}/\partial T_g$ is the slope of the straight lines in Figure 6. Values of $T_{den}(f \rightarrow \infty)$ and of $\partial T_{den}/\partial T_g$ obtained from a linear fit are reported in Table 2.

Note that the straight line for trehalose lies above that relative to sucrose; that is, trehalose acts as a better stabilizer than sucrose in systems having equal glass transition temperatures. Plots in Figure 6a suggest that collective water/disaccharide interactions, responsible for the glass transition, also influence the protein denaturation; however, the plots show that other effects must play a role in the “trehalose peculiarity”. Indeed,

at the same T_g value, trehalose is more effective than sucrose against thermal denaturation.

By inserting eq 1 into eq 2, T_{den} can be expressed as a function of the water/disaccharide mole ratio (f) as follows:

$$T_{den}(f) = T_{den}(f \rightarrow \infty) + \frac{\partial T_{den}}{\partial T_g} \frac{T_g(f \rightarrow 0) - T_g(f \rightarrow \infty)}{1 + k \left(\frac{MW_w}{MW_s} f \right)} \quad (3)$$

This expression shows how the tight relationship between the glass transition properties and the protein stability depends on both the water content and the particular nonreducing disaccharide used as a biopreserver. Note that all the quantities appearing in eq 3 can be determined experimentally. For trehalose and sucrose, eq 3 reads, respectively,

$$T_{den}(f) = 346.6 + \frac{17.5}{1 + 0.1f} \text{ (in Kelvin)}$$

and

$$T_{den}(f) = 345.0 + \frac{14.6}{1 + 0.1f} \text{ (in Kelvin)}$$

The lines in Figure 3a are the fitting of eq 3 to the experimental points, and as evidenced in the figure, the agreement with the experimental data is excellent. This implies that, in addition to the result that, at low hydrations, the denaturation temperature of the protein is related to the glass forming properties of the whole water–disaccharide–protein matrix, eq 3 has also “practical” consequences in that the stability of myoglobin can be predicted from the calorimetric properties of the ternary system. If extended to other relevant proteins, this could be an important result in the field of biopreservation.

At variance with nonreducing disaccharides, in both maltose and lactose, the T_{den} -vs- T_g data exhibit erratic behavior (Figure 6b). This is a consequence of the erratic behavior observed in the protein denaturation temperatures (see Figure 3b). This behavior in the hydration dependence of denaturation temperature (but not of the glass transition temperature; see Figure 5c–d) suggests the existence of different denaturation processes. In this respect, the Maillard reaction has to be taken into account when dealing with reducing disaccharides.^{58,59} In this process, the reducing group of the saccharide might condense with aminoacidic amino groups, yielding, through iminic intermediates, glycosylamines. These undergo Amadori rearrangement to ketosamines, which further react, leading to a wide, poorly characterized spectrum of either short-chain hydrolytic products or high molecular weight brown polymeric compounds, generically called melanoidines, whose precise identity strongly depends on the system composition and the conditions under which the process takes place. With the formation of the latter, intensive molecular cross-bridging might happen, with strong alterations of the thermodynamic properties of the whole system. Observations on maltose–water matrixes of glycine under conditions analogous to our protein–disaccharide–water samples (data not shown) indicate that the Maillard reaction gives no sharp DSC signal: this explains why its presence is not evident in our calorimetric upscans. We ascribe the erratic behavior of the data in the T_{den} -vs- f and T_{den} -vs- T_g plots for reducing disaccharide systems (Figures 3b and 6b) to the denaturation

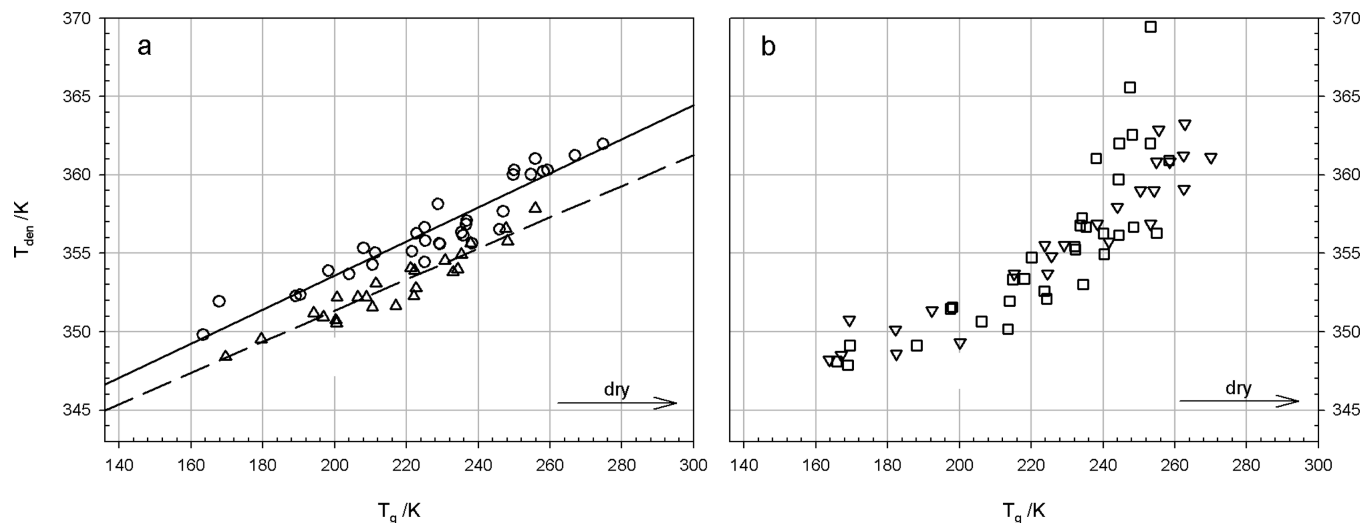


Figure 6. Denaturation temperature of myoglobin as a function of glass transition temperature. Panel a: trehalose⁴⁸ and sucrose. Panel b: maltose and lactose. Symbols as in Figure 3. Lines in panel a are linear fittings.

TABLE 2: Parameters Obtained from Linear Fittings of T_{den} vs. T_g with Eq 2 in the Text

disaccharide	$T_{\text{den}}(f \rightarrow \infty)/\text{K}$	$\partial T_{\text{den}}/\partial T_g$
trehalose	346.6 ± 1.5	0.109 ± 0.016
sucrose	345.0 ± 1.3	0.099 ± 0.015

of protein–disaccharide complexes in which the protein has already undergone Maillard reaction. It has to be pointed out that the Maillard process has a complex dependence on water activity, with different effects on each elementary step. Hence, the erratic behavior during dehydration could be expected, and the apparently disordered onset of the protein denaturation temperature can be accepted. In any case, data in Figures 3b and 6b confirm that reducing disaccharides cannot be used in protein preservation, no matter the involved mechanism.

Conclusions

The protein–matrix structure dynamics has been studied in previous FTIR experiments⁶⁰ on very dry MbCO–trehalose–water systems. In these experiments was studied the temperature dependence, 300–20 K, of the CO stretching band (whose thermal evolution reflects the interconversion among protein taxonomic A substates⁶¹) and of the water association band⁶² (whose thermal evolution reflects thermal behavior of the matrix). Results showed that as a counterpart of the effects of the trehalose matrix on the structure of the embedded protein, the presence of the protein influences the structure of the trehalose/water matrix, indicating a protein–matrix coupling over the whole temperature range explored. This led to the prediction⁶⁰ of an effect of the embedded protein on the glass transition temperature of the ternary system.

Here, we studied (1) the glass transition of binary disaccharide–water and ternary protein–disaccharide–water systems and (2) the relationship between the glass transition temperature of the ternary system and the temperature of thermal denaturation of the embedded protein in nonreducing (trehalose, sucrose) and reducing (maltose, lactose) disaccharides. Results showed that the presence of the protein lowers the glass transition temperature for all the disaccharides investigated. This is in line with the mentioned simulative⁴¹ and FTIR results,⁶⁰ which showed that at low water content, the protein competes for water with disaccharide molecules, thus reducing the strength of the HB network encompassing the sample. Furthermore, the

denaturation temperature of the protein is found linearly correlated to the glass transition temperature of the protein–water–disaccharide matrix, at least in nonreducing disaccharides. This indicates that the collective properties of the matrix that regulate the glass transition are linearly correlated to local properties that determine the denaturation of the protein, whose temperature increase with disaccharide concentration is entropy-driven.

References and Notes

- (1) Fox, K. C. *Science* **1995**, *267*, 1922–1923.
- (2) Timasheff, S. N. *Biochemistry* **2002**, *41*, 13474–13482.
- (3) Crowe, L. M. *Comp. Biochem. Phys. A* **2002**, *131*, 505–513.
- (4) Crowe, J. H. *Adv. Exp. Med. Biol.* **2007**, *594*, 143–158.
- (5) Jain, N. K.; Roy, I. *Protein Sci.* **2008**, *18*, 24–36.
- (6) Carpenter, J. F.; Crowe, J. H. *Biochemistry* **1989**, *28*, 3916–3922.
- (7) Sum, A. K.; Faller, R.; de Pablo, J. J. *Biophys. J.* **2003**, *85*, 2830–2844.
- (8) Pereira, C.; Lins, R. D.; Chandrasekhar, I.; Freitas, L. C. G.; Hunenberger, P. H. *Biophys. J.* **2004**, *86*, 2273–2285.
- (9) Villarreal, M. A.; Dyaz, S. B.; Disalvo, E. A.; Montich, G. G. *Langmuir* **2004**, *20*, 7844–7851.
- (10) Pereira, C.; Hunenberger, P. H. *J. Phys. Chem. B* **2006**, *110*, 15572–15581.
- (11) Belton, P. S.; Gil, A. M. *Biopolymers* **1994**, *34*, 957–961.
- (12) Timasheff, S. N. *Adv. Protein Chem.* **1998**, *51*, 355–432.
- (13) Sampedro, J. G.; Uribe, S. *Mol. Cell. Biochem.* **2004**, *256*, 319–327.
- (14) Green, J. L.; Angell, C. A. *J. Phys. Chem.* **1989**, *93*, 2880–2882.
- (15) Hagen, J.; Hofrichter, J.; Eaton, W. A. *Science* **1995**, *269*, 959–962.
- (16) Gottfried, D. S.; Peterson, E. S.; Sheikh, A. G.; Wang, J.; Yang, M.; Friedman, J. M. *J. Phys. Chem.* **1996**, *100*, 12034–12042.
- (17) Sastry, G. M.; Agmon, N. *Biochemistry* **1997**, *36*, 7097–7108.
- (18) Kleinert, T.; Doster, W.; Leyser, H.; Petry, W.; Schwarz, V.; Settles, M. *Biochemistry* **1998**, *37*, 717–733.
- (19) Lichtenegger, H.; Doster, W.; Kleinert, T.; Birk, A.; Sepiol, B.; Vogl, G. *Biophys. J.* **1999**, *76*, 414–422.
- (20) Schlichter, J.; Friedrich, J.; Herenyi, L.; Fidy, J. *Biophys. J.* **2001**, *80*, 2011–2017.
- (21) Ponkratov, V. V.; Friedrich, J.; Vanderkooi, J. M. *J. Chem. Phys.* **2002**, *117*, 4594–4601.
- (22) Mei, E.; Tang, J.; Vanderkooi, J. M.; Hochstrasser, J. M. *J. Am. Chem. Soc.* **2003**, *125*, 2730–2735.
- (23) Caliskan, G.; Mechtani, D.; Roh, J. H.; Kisliuk, A.; Sokolov, A. P.; Azzam, S.; Cicerone, M. T.; Lin-Gibson, S.; Peral, I. *J. Chem. Phys.* **2004**, *121*, 1978–1983.
- (24) Massari, A. M.; Finkelstein, I. J.; McClain, B. L.; Goj, A.; Wen, X.; Bren, K. L.; Loring, R. F.; Fayer, M. D. *J. Am. Chem. Soc.* **2005**, *127*, 14279–14289.
- (25) Massari, A. M.; Finkelstein, I. J.; Fayer, M. D. *J. Am. Chem. Soc.* **2006**, *128*, 3990–3997.
- (26) Samuni, U.; Dantsker, D.; Roche, C. J.; Friedman, J. M. *GENE* **2007**, *398*, 234–248, and references therein.

- (27) Cordone, L.; Cottone, G.; Giuffrida, S.; Palazzo, G.; Venturoli, G.; Viappiani, C. *Biochim. Biophys. Acta* **2005**, *1749*, 252–281, and references therein.
- (28) Giuffrida, S.; Cottone, G.; Cordone, L. *Biophys. J.* **2006**, *91*, 968–980, and references therein.
- (29) Cordone, L.; Cottone, G.; Giuffrida, S. *J. Phys. Condens. Matter* **2007**, *19*, 205110, and references therein.
- (30) Cordone, L.; Cottone, G.; Giuffrida, S.; Librizzi, F. *Chem. Phys.* **2008**, *345*, 275–282, and references therein.
- (31) Cottone, G.; Cordone, L.; Ciccotti, G. *Biophys. J.* **2001**, *80*, 931–938.
- (32) Francia, F.; Palazzo, G.; Mallardi, A.; Cordone, L.; Venturoli, G. *Biochim. Biophys. Acta* **2004**, *1658*, 50–57, and references therein.
- (33) Francia, F.; Dezi, M.; Mallardi, A.; Palazzo, G.; Cordone, L.; Venturoli, G. *J. Am. Chem. Soc.* **2008**, *130*, 10240–10246.
- (34) Giachini, L.; Francia, F.; Cordone, L.; Boscherini, F.; Venturoli, G. *Biophys. J.* **2007**, *92*, 1350–1360.
- (35) Francia, F.; Malferrari, M.; Sacquin-Mora, S.; Venturoli, G. *J. Phys. Chem. B* **2009**, in press.
- (36) Librizzi, F.; Vitrano, E.; Cordone, L. Inhibition of A Substates Interconversion in Trehalose Coated Carbonmonoxy-Myoglobin. In *Biological Physics*; Frauenfelder, H., Hummer, G., Garcia, R., Eds.; AIP American Institute of Physics: Melville, New York, 1999; pp 132–138.
- (37) Librizzi, F.; Viappiani, C.; Abbruzzetti, S.; Cordone, L. *J. Chem. Phys.* **2002**, *116*, 1193–1200.
- (38) Schirò, G.; Cupane, A. *Biochemistry* **2007**, *46*, 11568–11576.
- (39) Schirò, G.; Sclafani, M.; Caronna, C.; Natali, F.; Plazanet, M.; Cupane, A. *Chem. Phys.* **2008**, *345*, 259–266.
- (40) Schirò, G.; Sclafani, M.; Natali, F.; Cupane, A. *Eur. Biophys. J.* **2008**, *37*, 543–549.
- (41) Cottone, G.; Ciccotti, G.; Cordone, L. *J. Chem. Phys.* **2002**, *117*, 9862–9866.
- (42) Cottone, G. *J. Phys. Chem. B* **2007**, *111*, 3563–3569.
- (43) Doster, W.; Bacheitner, A.; Dunau, R.; Hiebl, M.; Luscher, E. *Biophys. J.* **1986**, *50*, 13–219.
- (44) Tarek, M.; Tobias, D. J. *Biophys. J.* **2000**, *79*, 3244–3257.
- (45) Tarek, M.; Tobias, D. J. *Phys. Rev. Lett.* **2002**, *88*, 8101–8104.
- (46) Rector, D.; Jiang, J.; Berg, M. A.; Fayer, M. D. *J. Phys. Chem. B* **2001**, *105*, 1081–1092.
- (47) Lam, Y. H.; Bustami, R.; Phan, T.; Chan, H. K.; Separovic, F. *J. Pharm. Sci.* **2002**, *91*, 943–951.
- (48) Bellavia, G.; Cordone, L.; Cupane, A. *J. Therm. Anal. Calorim.* **2009**, *95*, 699–702.
- (49) Takahashi, K.; Sturtevant, J. M. *Biochemistry* **1981**, *20*, 6185–6190.
- (50) Bell, L. N.; Hageman, M. J.; Bauer, J. M. *Biopolymers* **1995**, *35*, 201–209, and references therein.
- (51) Xie, G.; Timasheff, S. N. *Biophys. Chem.* **1997**, *64*, 25–43.
- (52) Roos, Y. J. *J. Therm. Anal. Calorim.* **1997**, *48*, 535–544.
- (53) Gordon, M.; Taylor, J. S. *J. Appl. Chem.* **1952**, *2*, 493–500.
- (54) Hallbrucker, A.; Mayer, E.; Johari, G. P. *J. Phys. Chem.* **1989**, *93*, 4986–4990.
- (55) Roos, Y. *Carbohydr. Res.* **1993**, *238*, 39–48.
- (56) Miller, D. P.; dePablo, J. J. *J. Phys. Chem. B* **2000**, *104*, 8876–8883, and references therein.
- (57) Cesàro, A.; De Giacomo, O.; Sussich, F. *Food Chem.* **2008**, *106*, 1318–1328.
- (58) Ledl, F.; Schleicher, E. *Angew. Chem., Int. Ed.* **1990**, *29*, 565–706.
- (59) Kwak, E. J.; Lim, S. I. *Amino Acids* **2004**, *27*, 85–90.
- (60) Giuffrida, S.; Cottone, G.; Librizzi, F.; Cordone, L. *J. Phys. Chem. B* **2003**, *107*, 13211–13217.
- (61) Frauenfelder, H.; Parak, F.; Young, R. D. *Annu. Rev. Biophys. Chem.* **1988**, *17*, 451–479.
- (62) Eisenberg, D.; Kauzmann, W. *The Structure and Properties of Water*; Oxford University Press: London, 1969.

JP9041342